Available online at www.sciencedirect.com
ScienceDirect
Journal of Sound and Vibration 304 (2007) 361–381
JOURNAL OF SOUND AND VIBRATION
www.elsevier.com/locate/jsvi

Slosh dynamics of liquid-filled containers with submerged components using pressure-based finite element method

S. Mitra*, K.P. Sinhamahapatra

Department of Aerospace Engineering, IIT Kharagpur, West Bengal 721302, India

Received 22 March 2006; received in revised form 29 January 2007; accepted 4 March 2007

Abstract

Seismic response of liquid storage tank can be strongly influenced by the presence of submerged components. This modification of the dynamic characteristics of the liquid tank systems with internal components can be very useful for improving their seismic behavior. In this paper, a pressure-based finite element technique has been developed to analyze the slosh dynamics of a partially filled rigid container with bottom-mounted submerged components. The fluid is assumed homogeneous, isotropic, inviscid, and to exhibit only limited compressibility. The problem is linearized assuming the frequency of the exciting oscillation not in the immediate neighborhood of the natural slosh frequency, so that the slope of the free surface is small. The linearized problem is spatially discretized using the Galerkin weighted residual method. Earthquake excitations are used as the prescribed boundary condition. The solution is advanced in time using Newmark's constant average acceleration method. The developed code has been used to investigate the effect of a bottom-mounted rectangular component on the slosh dynamics of a liquid-filled rigid container. Numerical results obtained are compared with the existing solutions to validate the code. The parametric study of the tank–fluid system shows the importance of height, width and location of the submerged structural components.

1. Introduction

Sloshing is a potential source of disturbance in liquid storage containers. The motion of liquids in rigid containers has been the subject of many studies in the past few decades because of its frequent application in several engineering disciplines as exemplified by fuel sloshing in liquid propellant launch vehicles, aircrafts, and suspension bridges, oil oscillation in large storage tanks, water oscillation in a reservoir and sloshing in the nuclear fuel storage pool due to earthquake and similar other situation, and in biomechanical systems. Although the problem is generally nonlinear, the linearization of the system can give satisfactory results in many cases, such as the interaction of small structure motions with acoustic waves in fluids (acoustoelastic fluid–structure interaction model). Two formulations are mainly practiced, both using the displacements as the unknowns for the structure. For the fluid, the unknowns are either the displacements, or a force-like quantity, such as the pressure or the velocity potential or the displacement potential. The sloshing response of the

*Corresponding author. Tel.: +91 3222 283018; fax: +91 3222 282242/255303.
E-mail addresses: rssmitra@aero.iitkgp.ernet.in, aero_mitra@yahoo.com (S. Mitra).

0022-460X/$ - see front matter © 2007 Elsevier Ltd. All rights reserved.
doi:10.1016/j.jsv.2007.03.014

Nomenclature

a	position of the block (distance of left wall of the block from the left wall of the tank)
B_f	liquid free surface boundary
B_{cb}	bottom boundary of the component
B_{cw}	interface boundary between component wall and the fluid
B_{tb}	bottom boundary of the tank
B_{tw}	interface boundary between tank wall and the fluid
c	velocity of sound in the fluid medium
g	acceleration due to gravity
$\mathbf{K}_f$	fluid stiffness matrix
$\mathbf{M}_f$	fluid mass matrix
N_i	interpolation function
$\bar{p}$	nodal pressure
$\dot{p}$	variation of pressure with respect to time
p	hydrodynamic pressure in excess of the hydrostatic pressure
$\ddot{u}_n$	normal component of the structural acceleration
w	width of the block
ρ_f	density of the fluid

fluid–structure system is found to be very sensitive to the characteristics of the ground motion and configuration of the system [1–7]. For ground excitation dominated by low-frequency contents, the sloshing response increases significantly and the contribution of the higher sloshing modes increases [2]. To understand the dynamic behavior of the liquid storage tanks and to provide proper design codes, many research groups have concentrated their investigation on the seismic behavior of the liquid containers and on the earthquake resistant design. Regarding the importance of these systems, specially their seismic safety for avoiding the adverse consequences such as fire, explosions, structural failure, environment pollution, better understanding of their seismic behavior is still necessary. In spite of the continuous efforts to enhance the performance of liquid containers against seismic loading, many liquid tanks have been severely damaged in major earthquakes all over the world. The field studies report that liquid-filled containers are usually damaged due either to excessive axial compression caused by overall bending of the containers or to sloshing of the contained liquid with insufficient freeboard between the liquid surface and the tank roof [8]. Since the earthquakes are unpreventable and unpredictable the only course open to the engineers is to design and built the fluid–structure system so that the loss of property and life can be minimized. Particularly for the spent nuclear fuel storage pool, clear understanding of sloshing phenomena is required for finding freeboard and to prevent overflow, and for the estimation of hydrodynamic pressure on the pool and submerged components. The spent nuclear fuel storage pool structure should assure the safety of the stored spent fuels and its structural integrity against design earthquake loads. The presence of equipments or components submerged in the liquid may significantly change the dynamic response of the fluid–structure systems. Although there have been numerous studies on the sloshing behavior in fluid–structure systems, there are a limited number of studies reported on the sloshing response in a liquid tank with single or multiple submerged components. Choun and Yun [1,2] have presented an elegant analytical treatment of rectangular tanks with a submerged structure using potential formulation and small-amplitude water wave theory and have observed that under a typical earthquake submerged structure shows a tendency to decrease the sloshing amplitude and hydrodynamic pressure. Watson and Evans [9] studied the sloshing frequencies of a rectangular tank system containing a partially or fully submerged rectangular block, centrally mounted on the floor, using eigenfunction and Galerkin expansions approaches.

The focus of this study is to provide the engineers with a set of tools to accurately and efficiently model the slosh dynamics phenomena with particular reference to the classic acoustoelastic sloshing problem of a liquid-filled container with submerged component experiencing seismic excitation. In the present study the characteristics of slosh displacement, slosh frequencies and mode shapes and the hydrodynamic pressure over the container wall and around the submerged component for a prescribed excitation have been addressed for rectangular containers. The present study also investigates the effects of height, width and location of an internal block on the sloshing characteristics and dynamic responses. The fluid domain is discretized using

4-noded quadrilateral elements with pressure as the degree of freedom. The problem is formulated using the Galerkin's principle, which provides the basis for the present discretization. Newmark's constant average acceleration technique, a finite difference based iterative time stepping scheme, is employed to advance the solution in the time domain. Numerical results for the rigid containers with a bottom-mounted rectangular component are compared with available existing solutions. Through comprehensive parametric studies of the systems with submerged component, the present analyses attempt to elucidate the underlying response mechanism and the effects and relative importance of the parameters involved. The characteristics of sloshing behavior, primarily liquid frequencies, mode shapes and forced response characteristics have been studied in this paper. The results indicate that the size and the location of the component significantly influence the slosh response characteristics.

Since early 1950s several researchers have studied the linear slosh models for simple geometries. This study presents a numerical method for two-dimensional sloshing analysis of rectangular liquid storage tanks with a submerged component using a pressure-based finite element formulation and the linearized water wave theory. Usually compressibility proves to be negligible in the general linearized theory of waves on a homogeneous body of liquid. The examples presented in this paper fall in that category. However, in many practical cases as in the waste storage tanks and spent fuel reprocessing tanks in nuclear facilities, the fluid is inhomogeneous and the density variation is non-uniform but considerable. For the fluid–structure interaction problems, Muller [10] has shown mathematically that eigenvalues of a structure in contact with a compressible fluid are lower than the corresponding eigenvalues if the fluid were incompressible. Further, a numerical example is also presented to establish the same considering both air and water as the working fluid. Since compressibility can be included without considerable complexity and cost within the framework of linearized pressure-based formulation, the compressibility is included in this study for a probable future application where compressibility should not be neglected.

2. Governing equations and formulation

A pressure-based formulation has been considered in the present study. The linearized governing equation for an inviscid, compressible, irrotational flow in terms of excess pressure variable $p(x, z, t)$ is the well-known wave equation [11], written as

$$\nabla^2 p(x,z,t) = \frac{1}{c^2}\ddot{p}(x,z,t) \quad \text{in } \Omega. \tag{1}$$

The pressure formulation has certain advantages over the displacement or velocity potential based formulations. Unlike the displacement formulation, the number of unknown in this formulation is only one per node (pressure), which results in considerable saving of computer storage and time, particularly for large three-dimensional problems. Also, the pressure field at the structure–fluid interface is directly obtained unlike other methods where the pressure has to be calculated from velocity or displacement or their potential. This would be particularly advantageous in solving a fluid–structure interaction problem where pressure on the interface need to be computed at each time step. Besides these major advantages, the compressibility comes in a natural way in a pressure formulation and can be retained without incurring considerable additional efforts and cost.

The fluid boundary, in general, is composed of three types of boundaries. These are solid–liquid interface boundary, free surface boundary, non-reflecting or radiating type boundary. For liquid sloshing in a container the radiating type boundary is neglected. The appropriate boundary conditions for these boundaries are as follows:

1. *Solid– liquid interface boundary*: Continuity of normal displacement at the solid–liquid interface leads to the following relation for the linearized problem:

$$\frac{\partial p}{\partial n} = -\rho_f \ddot{u}_n \quad \text{on } B_{\text{tw}} \text{ and } B_{\text{cw}}. \tag{2}$$

2. *Free surface boundary*: The linearized wave theory [12] facilitates the satisfaction of the free surface boundary condition on the undisturbed free surface. The free surface boundary conditions are linearized to give

$$p = \rho_f g u_n, \tag{3a}$$

$$\frac{\partial p}{\partial n} = -\frac{\ddot{p}}{g} \quad \text{on } B_f. \tag{3b}$$

Eq. (3a) is used to deduce the free surface displacement.

3. *Bottom boundary*: Considering the bottom boundary to be rigid, at the bottom of the tank or component

$$\partial p/\partial n = 0 \quad \text{on } B_{\text{tb}} \text{ and } B_{\text{cb}}. \tag{4}$$

Here ρ_f, $\ddot{u}_n$ and g are the fluid density, structure's normal acceleration at the structure–fluid interface and acceleration due to gravity. For a rigid container, the structural acceleration $\ddot{u}_n$ is identical to the prescribed ground acceleration.

Applying divergence theorem to the residual form of the governing differential equation for the liquid and substituting Eqs. (2)–(4), one obtains

$$\int_\Omega \bar{N}^T \left[\frac{\partial^2 p}{\partial x^2} + \frac{\partial^2 p}{\partial y^2} - \frac{1}{c^2}\frac{\partial^2 p}{\partial t^2}\right] \mathrm{d}\Omega - \int_{B_{\text{tw+cw}}} \bar{N}^T \left[\frac{\partial p}{\partial n} + \rho_f \ddot{u}_n\right] \mathrm{d}\Gamma - \int_{B_f} \bar{N}^T \left[\frac{\partial p}{\partial n} + \frac{\ddot{p}}{g}\right] \mathrm{d}\Gamma - \int_{B_{\text{tb+cb}}} N^T \left[\frac{\partial p}{\partial n}\right] \mathrm{d}\Gamma = 0 \tag{5}$$

in which the total boundary $B = B_{\text{tw}} + B_f + B_{\text{tb}} + B_{\text{cw}} + B_{\text{cb}}$, is as defined in Fig. 1(a). Using Green–Gauss theorem and introducing the Galerkin finite element approximation the above equation reduces to the following set of algebraic equations:

$$\mathbf{M}_f \ddot{\bar{p}} + \mathbf{K}_f \bar{p} = \mathbf{F}, \tag{6}$$

where $\mathbf{M}_f$ is the mass matrix for a fluid element and is given by

$$(M_f)_{ij} = \frac{1}{c^2}\int_\Omega N_i^T N_j \,\mathrm{d}\Omega + \frac{1}{g}\int_{\Gamma_f} N_i^T N_j \,\mathrm{d}\Gamma. \tag{7}$$

Similarly, $\mathbf{K}_f$, the stiffness matrix for the fluid element, is given by

$$(K_f)_{ij} = \int_\Omega \left(\frac{\partial N_i}{\partial x}\frac{\partial N_j}{\partial x} + \frac{\partial N}{\partial y}\frac{\partial N_j}{\partial y}\right) \mathrm{d}\Omega \tag{8}$$

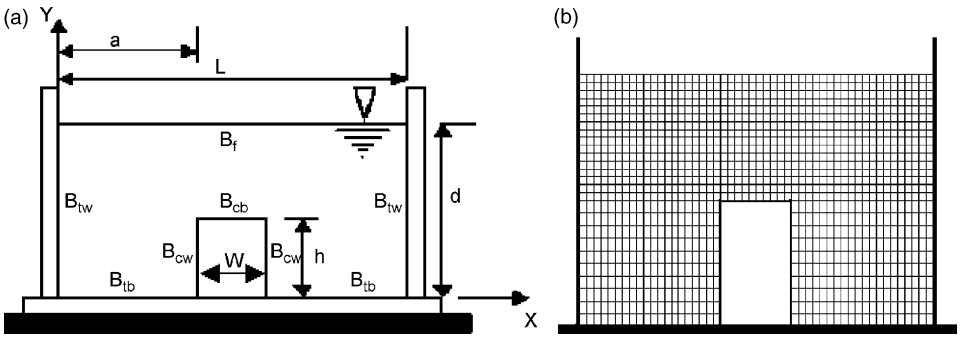

Fig. 1. (a) Problem configuration and nomenclature; (b) typical Mesh.

and the load vector **F** is

$$F_i = \int_{\Gamma_1} N_i^T \rho_f \ddot{u}_n \, d\Gamma. \tag{9}$$

For free vibration problems, the load vector **F** in Eq. (6) becomes zero.

The computation is carried out using 4-noded isoparametric fluid elements. A finer mesh is adopted near the free surface, where sloshing effects are more pronounced. A typical computational mesh is shown in Fig. 1(b). MATLAB [13] functions have been used to extract the eigenvalues and eigenvectors from the computed stiffness and mass matrices. Newmark's constant-average acceleration [14] technique has been used to solve the dynamic forced vibration equation. At each time step the set of algebraic equations are solved using a skyline LDL^{T} solver.

3. Numerical examples and discussion

Free vibration analyses are first carried out for a rectangular container with a rectangular block mounted at the bottom. Computations are performed with a 15 m wide block located at the center of the tank floor of a 30 m wide and 13 m deep (liquid depth) tank for several block heights (h). The computed frequencies against block height to liquid height ratios (h/d) are presented in Table 1 and are compared with those obtained by

Table 1
Sloshing frequencies of the tank system with a central block for different h/d ratio ($L = 30$ m, $d = 13$ m, $w = 15$ m)

h/d	ω_1 (rad/s)		ω_2 (rad/s)		ω_3 (rad/s)	
	Present	Choun and Yun [1]	Present	Choun and Yun [1]	Present	Choun and Yun [1]
0.	0.929	0.927	1.418	1.422	1.755	1.756
0.2	0.897	0.898	1.415	1.415	1.744	1.746
0.4	0.849	0.842	1.404	1.406	1.742	1.740
0.6	0.731	0.731	1.343	1.347	1.733	1.734
0.8	0.550	0.552	1.190	1.192	1.730	1.732

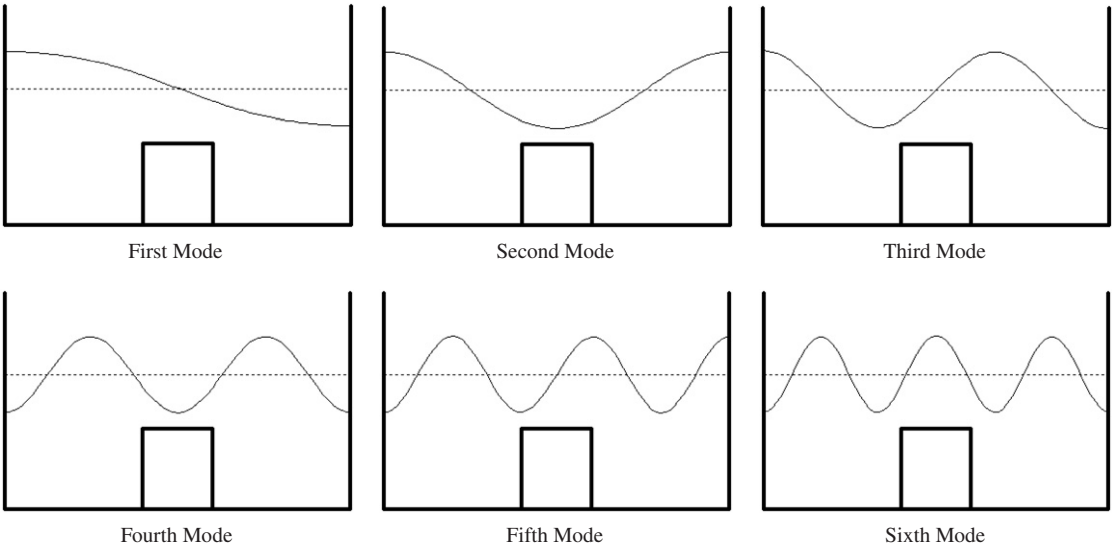

Fig. 2. Sloshing modes with a centrally located block ($h/d = 0.6$, $w/L = 0.2$).

Choun and Yun [1]. The results are found to be in excellent agreement. Choun and Yun [1] have also shown that their results are in very good agreement with those obtained from the ADINA [15] code. The reduction in the fundamental sloshing frequency with increase in the h/d ratio is quite noticeable. The decrease in higher mode frequencies is considerably less.

The corresponding first six natural sloshing mode shapes for the centrally located block ($a = 12\,\text{m}$, $w = 6\,\text{m}$ and $h = 7.8\,\text{m}$) are shown in Fig. 2. Similar mode shapes for a case with the block located off-center ($a = 6\,\text{m}$, $w = 3\,\text{m}$, $h = 7.8\,\text{m}$) are shown in Fig. 3. Comparison of the mode shapes could not be presented as the complete configuration of the cases reported in Ref. [1] are not available. However, it appears that the mode shapes agree quite well.

The sloshing responses of the tank system, subjected to the EW component of the El Centro earthquake (Fig. 4), are presented in the form of transient slosh wave height variation in Figs. 5(a)–(c) for $h/d = 0.0$, 0.5 and 0.8, respectively. The adopted tank system is 10 m wide having a liquid depth of 5 m. This particular tank system is considered for all the subsequent dynamic analyses reported in this paper. The rectangular block is located at the center ($a = 4\,\text{m}$, $w = 2\,\text{m}$ and $h = 3\,\text{m}$) for the computations in Fig. 5. The results clearly indicate a longer sloshing period when the submerged component is higher. The peak wave amplitude is found to reduce marginally with increase in the component height. The results are in reasonably good agreement with those obtained by Choun and Yun [2]. The differences in the peak values

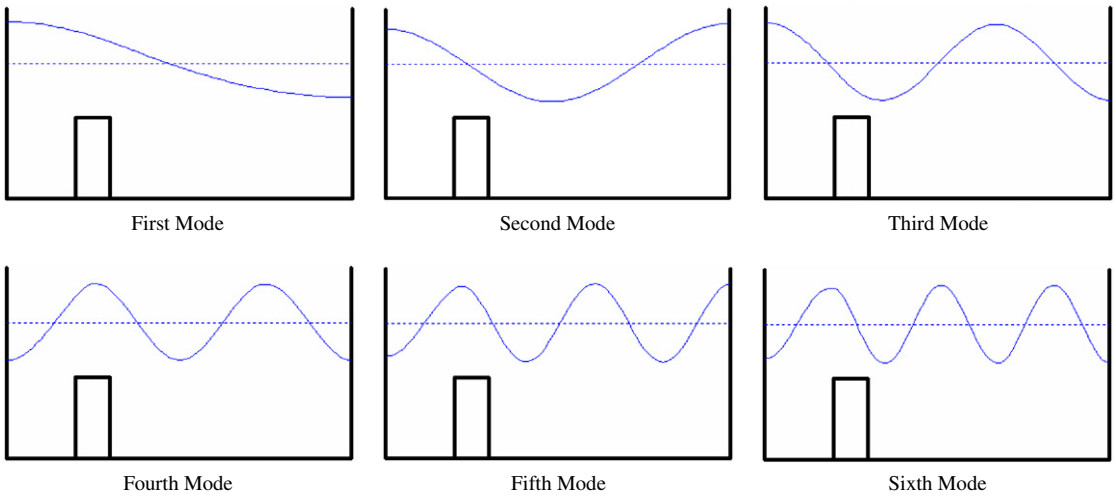

Fig. 3. Sloshing modes with an off-central block ($a/L = 0.2$, $h/d = 0.6$, $w/L = 0.1$).

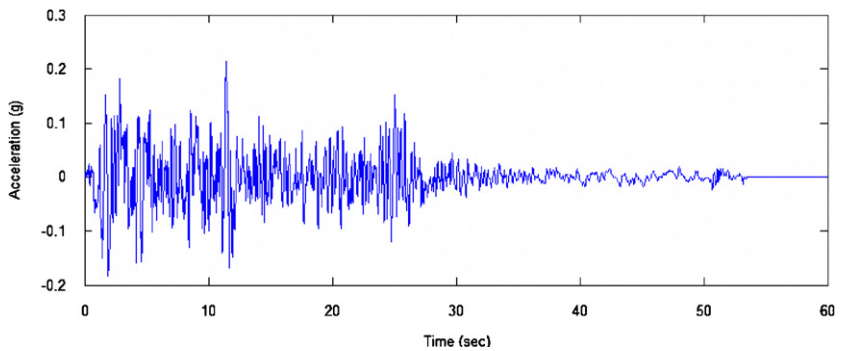

Fig. 4. The ground motion for the EW component of the El Centro earthquake.

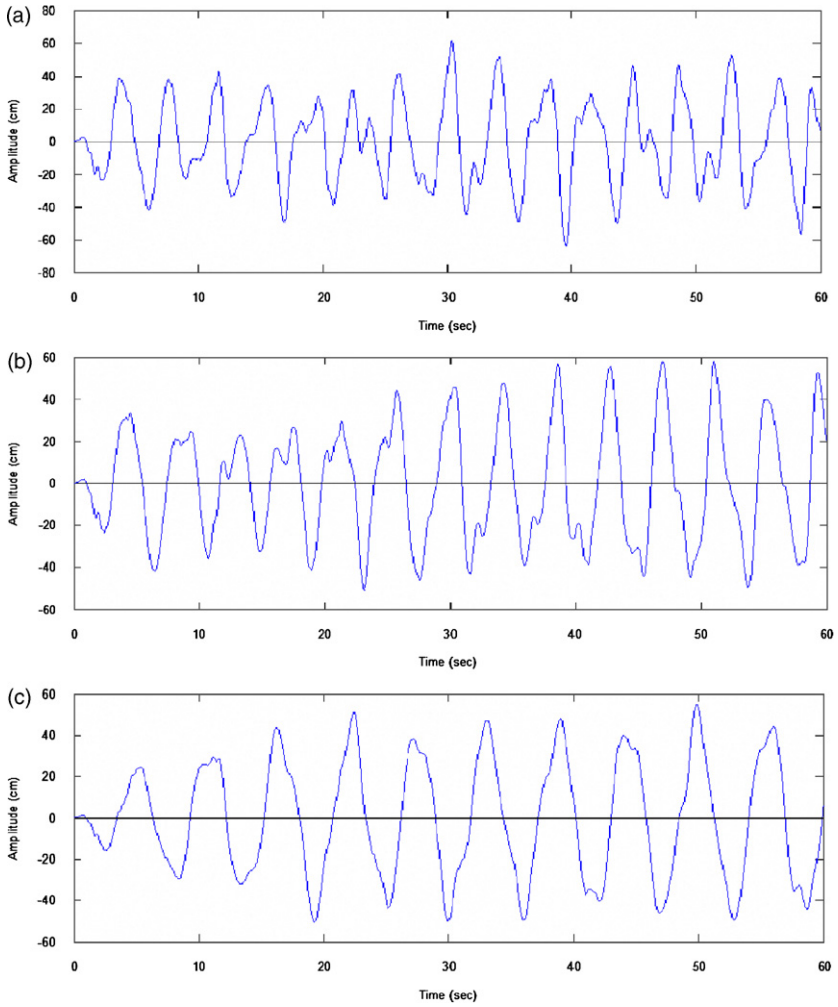

Fig. 5. Free surface displacement at $X = 0$ for different block heights: (a) $h/d = 0.0$, (b) $h/d = 0.5$, (c) $h/d = 0.8$.

may be attributed to the modal damping ratio of 0.005 that Choun and Yun [2] have considered in their analytic solution with 10 sloshing modes. The solutions due to Choun and Yun [2] are reproduced from the reference in Fig. 6.

A detailed parametric study of the slosh dynamic characteristics of the tank system is carried out to evaluate the influence of the size and location of the submerged block.

4. Slosh response due to change in the height of the block

Effect on sloshing characteristics of the tank system due to change in height of the submerged component has been studied keeping the width and location of the block fixed. A 2 m wide block ($w/L = 0.2$) located at the center is chosen to study the effect of h/d ratio. The input ground motion considered is the EW component of the El Centro earthquake.

Fig. 7 shows the transient pressure variation at the mean surface on the right wall of the tank for different submerged component height to depth of the liquid ratio, (h/d). It is observed from the figure that the pressure reaches to a maximum value of about 5892.5 Pa at 46.9 s for $h/d = 0.5$ and to 5529.5 Pa at 49.9 s for $h/d = 0.8$. Both the values are considerably smaller than the maximum pressure of 6250 Pa when the submerged

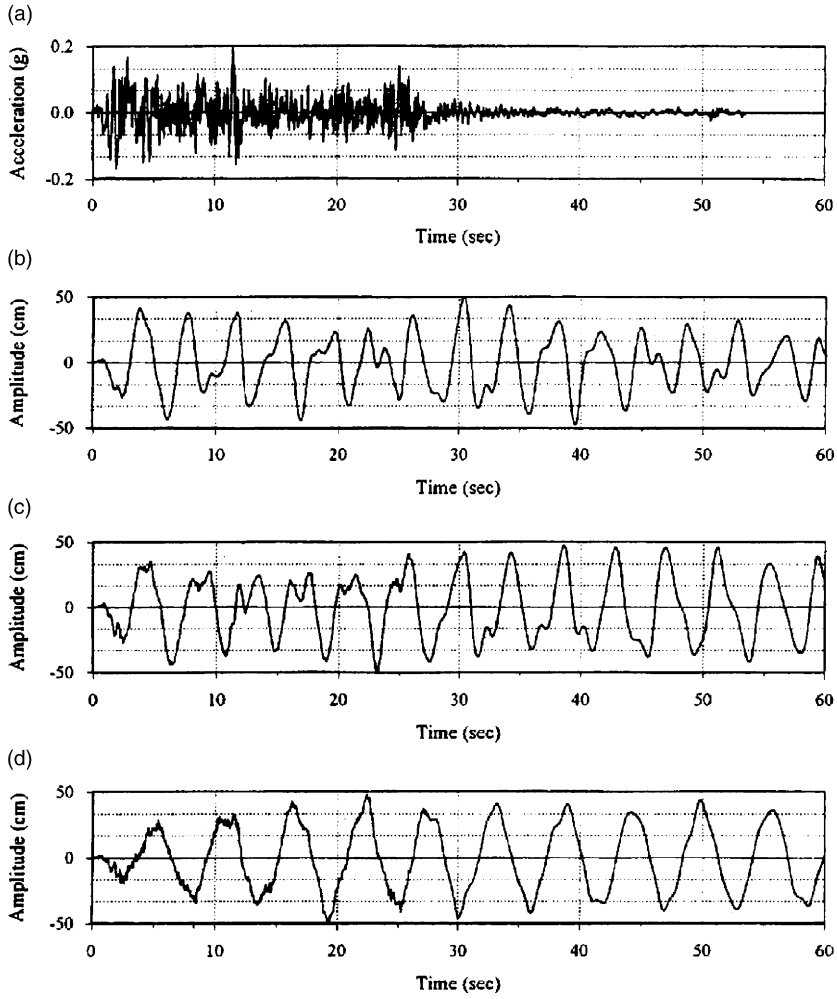

Fig. 6. Time histories of surface wave amplitude for various h/d ratios due to Choun et al. [2]. (a) ground motion, (b) $h/d = 0.0$, (c) $h/d = 0.5$, (d) $h/d = 0.8$.

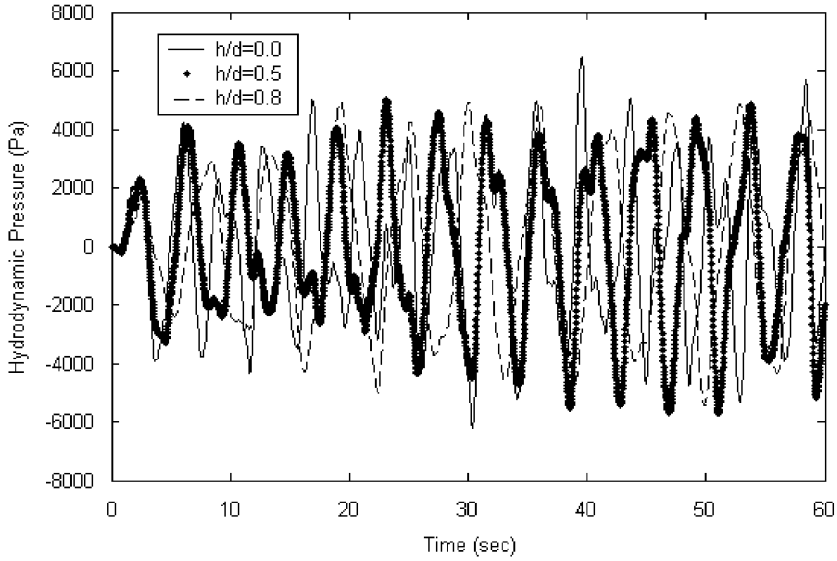

Fig. 7. Free surface hydrodynamic pressure variation with time.

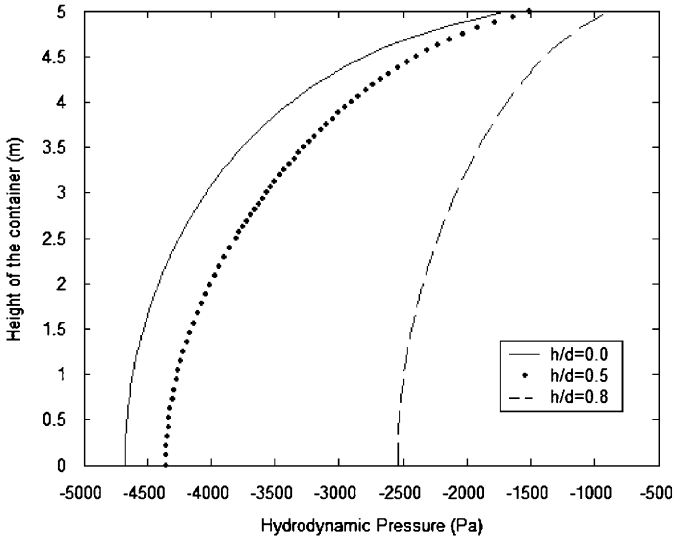

Fig. 8. Hydrodynamic pressure distribution along tank wall.

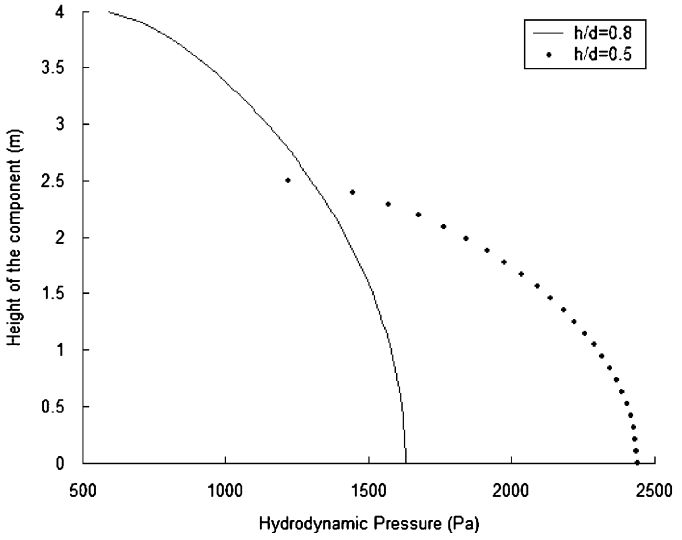

Fig. 9. Hydrodynamic pressure distribution along component wall.

component is absent. Also, in both the cases the peak occurs at a later instant, almost towards the termination of the excitation, compared to the no block case. Figs. 8 and 9 show the pressure distribution along the tank and the component wall at a particular time instant for various component heights. The temporal variations of hydrodynamic pressure at the top and bottom of the component wall are presented in Figs. 10 and 11. It is clearly evident from the figures that as the component height increase the maximum hydrodynamic pressure along the container wall decrease while the maximum pressure along the component wall increase. The increase in the peak hydrodynamic pressure along the component wall with increasing h/d is quite considerable. This also suggests an increase in the sloshing amplitude near the block with increasing h/d ratio.

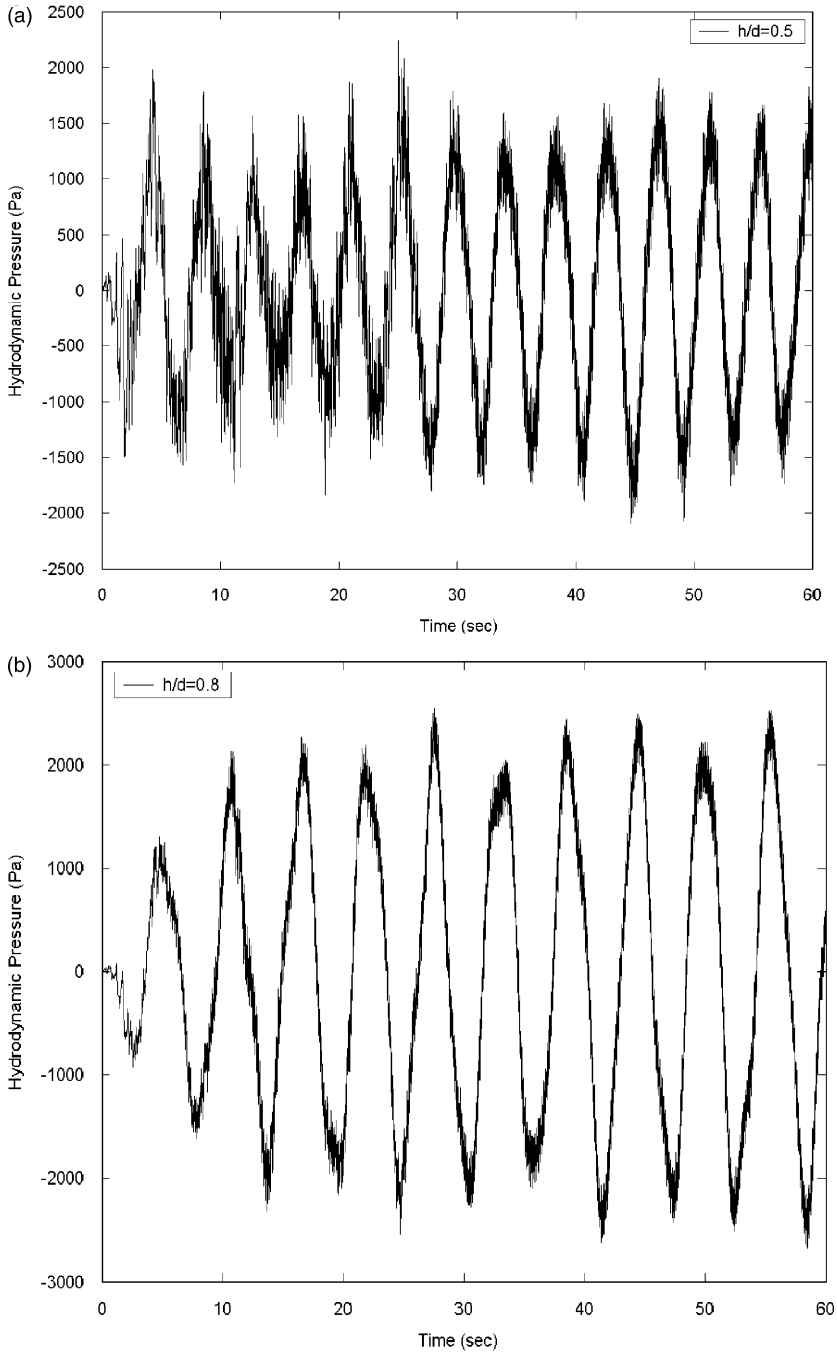

Fig. 10. Hydrodynamic pressure variation at top left corner of the component.

5. Slosh response due to location of the block

The transient variation of slosh wave amplitude at the free surface, due to EW component of the El Centro earthquake excitation, of the tank system with the submerged block placed at different location but width and height fixed at 2 and 2.5 m, respectively, is shown in Fig. 12. The figure shows that the slosh response is

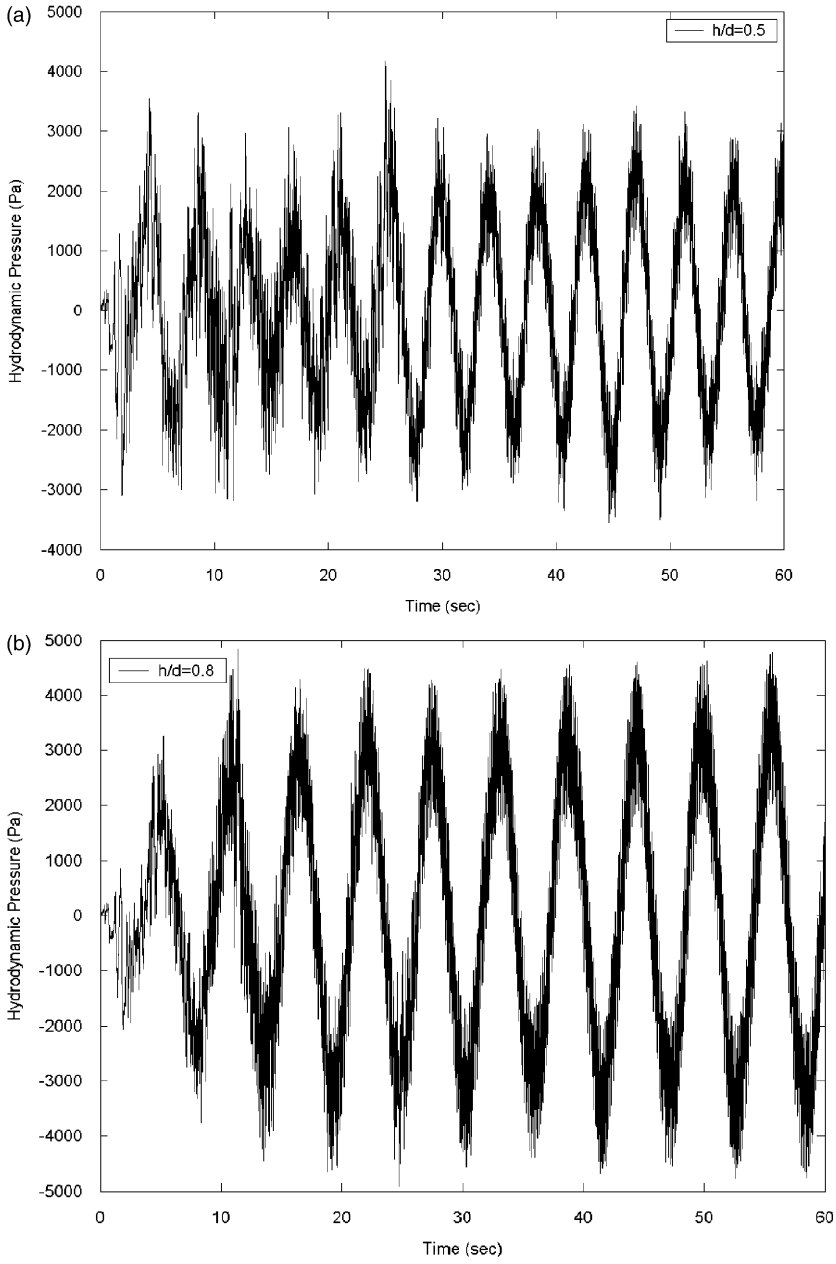

Fig. 11. Hydrodynamic pressure variation at bottom left corner of the component.

considerably affected by the location of the block for the case considered. The peak sloshing amplitude with an off-centered block appears to be nearly the same as with a centered block, but the peaks occur at different instants. It is found that the peaks for an off-centered block case occur around 20–25 s, while that for the centered block occur after 40 s, which is almost towards the termination of the excitation. Fig. 13 presents the slosh wave height at the left and right walls against time for $a = 2.5$ m ($a/L = 0.25$). It is found that maximum slosh wave height of nearly 56 cm occurs around 23 s. The hydrodynamic pressure variation along the left and right wall of the component and container are presented in Figs. 14–17. From Figs. 14(a) and (b) it can be seen that at a particular instant the hydrodynamic pressure on the two walls of the centrally located block are

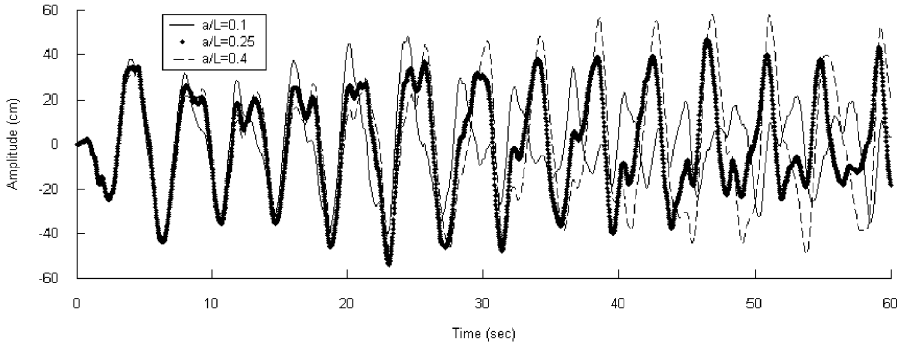

Fig. 12. Variation of slosh wave amplitude at $X = 0$ for different component locations.

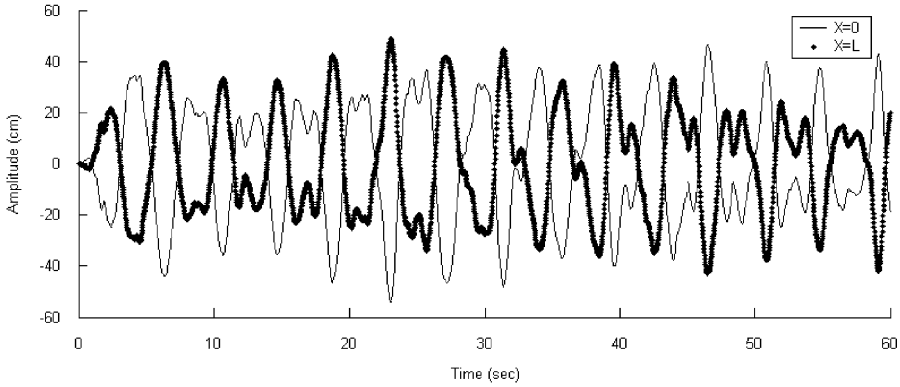

Fig. 13. Time histories of surface wave amplitude at the tank walls ($a/L = 0.25$).

nearly equal and opposite, giving rise to a zero hydrodynamic force. But when the block is placed towards the container wall, the pressure on the component walls acts in the same direction and a large hydrodynamic force acts on it. This situation prevails for most of the time of response. However, at some instances the pressures on the two component walls are opposing but their difference being quite considerable a large hydrodynamic force always acts on the block when it is very close to the tank wall. The variations of the hydrodynamic pressure at the top and bottom of the component wall are shown in Figs. 15 and 16. When the block is very close to the container wall, the pressure reaches a very high value during the early stages of the motion. The highest peak occurs almost at the same time when the ground motion has the highest peak. Subsequently, it falls down to more moderate values but still remains much larger than that due to a central or nearly central block. The reason may, perhaps, be attributed to the complex interaction between the propagating, reflected and scattered waves. The hydrodynamic pressure distributions at a particular instant along the left and right walls of the tank, shown in Figs. 17(a) and (b), indicates that pressure on the left wall (nearer to the block) increases as the block moves closer to it while the pressure on the right (far) wall reduces. The considerably large increase in the pressure on the near wall, up to the block height, when the block is very close to the wall ($a/L = 0.1$) is worth noting.

6. Slosh response due to change in width of the block

The same tank system is studied for the same prescribed excitation for different component width to the width of the tank ratio for a fixed component height of 2.5 m and liquid depth of 5 m. The block is located at the center of the tank floor. It is found from the results presented in Fig. 18 that with increasing w/L ratio the

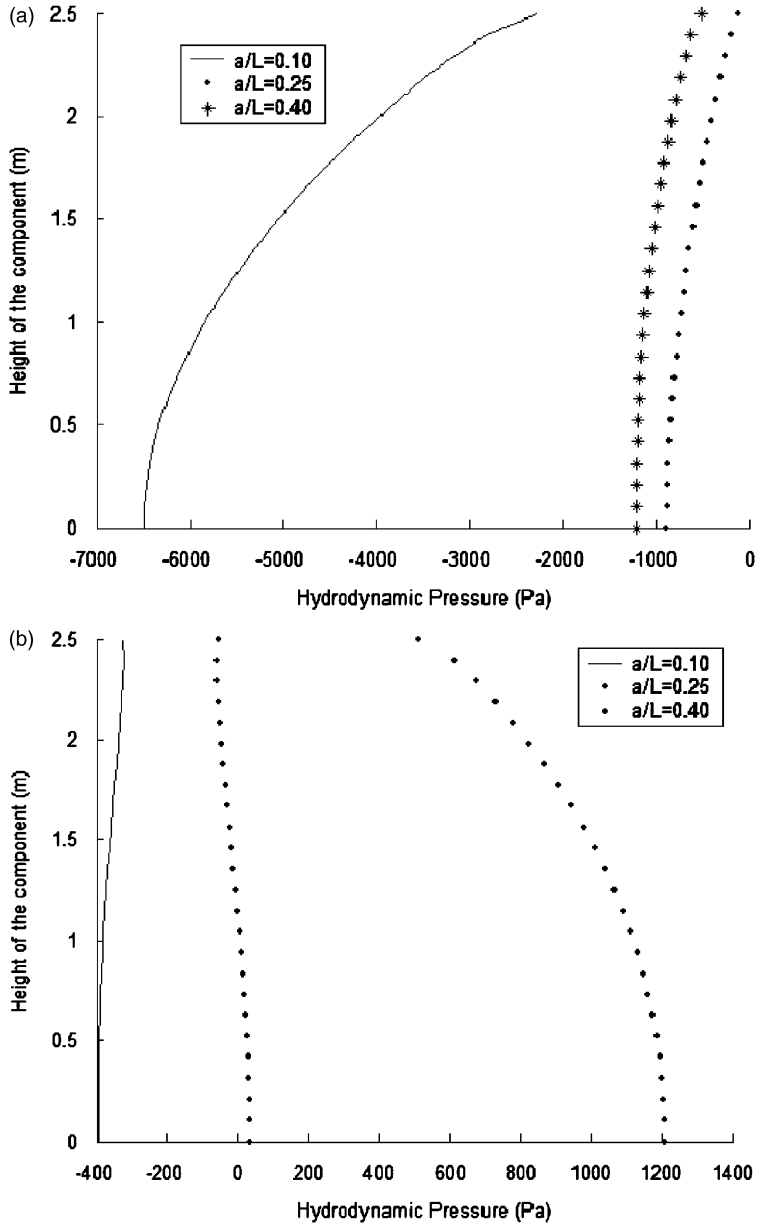

Fig. 14. Hydrodynamic pressure along component walls: (a) hydrodynamic pressure on the left wall of the component; (b) hydrodynamic pressure on the right wall of the component.

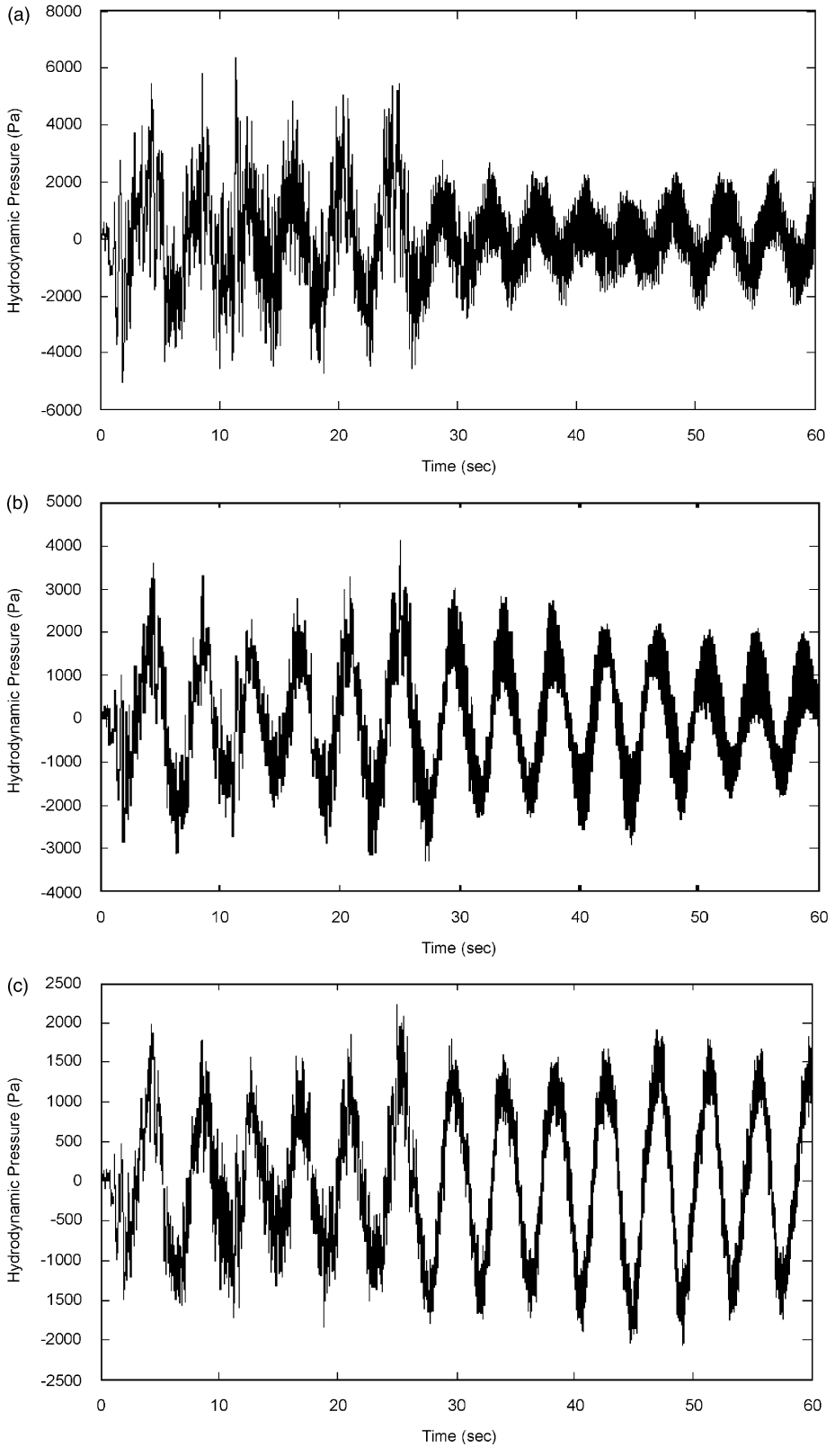

Fig. 15. Hydrodynamic pressure at the top left corner of the component: (a) $a/L = 0.1$, (b) $a/L = 0.25$, (c) $a/L = 0.40$.

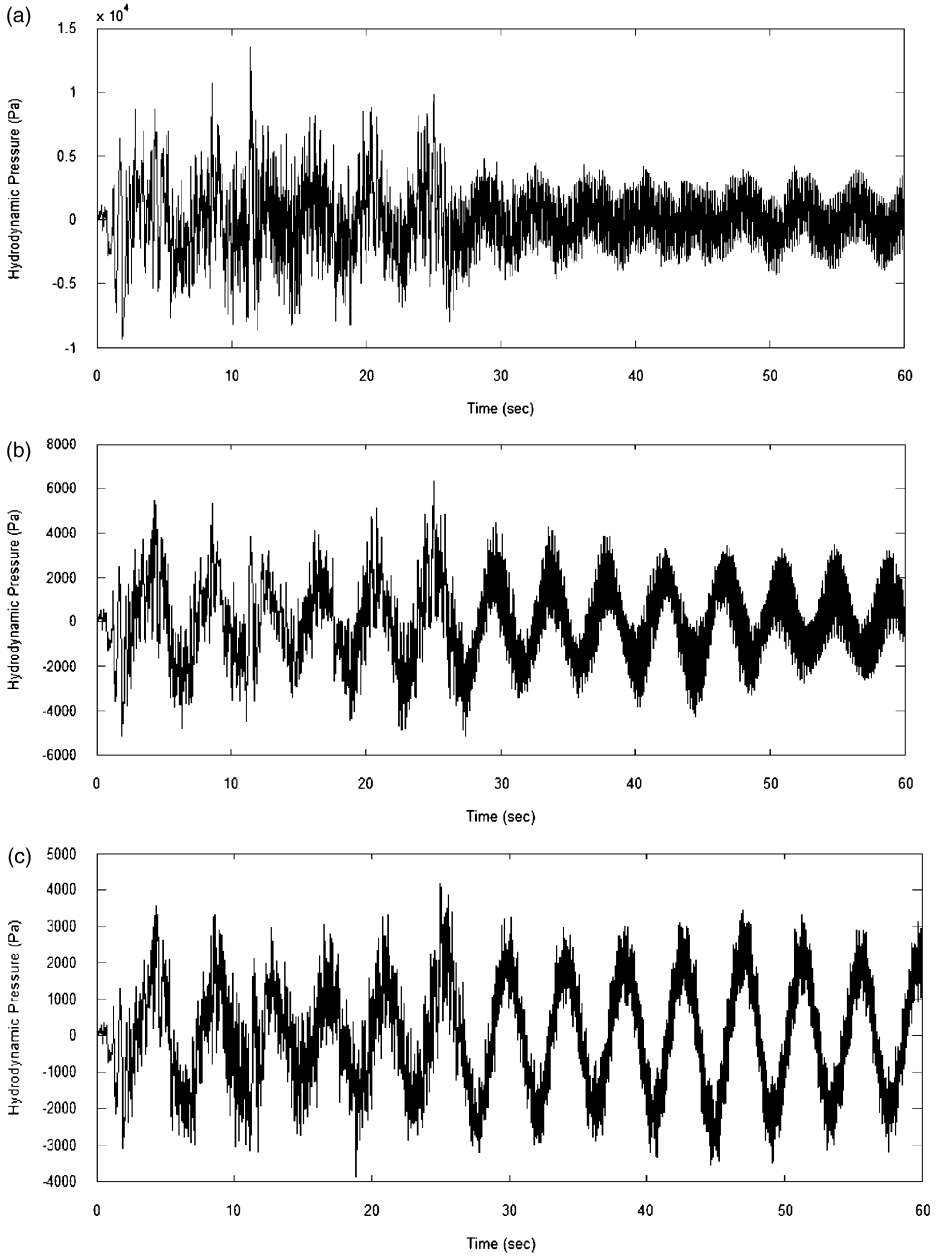

Fig. 16. Hydrodynamic pressure at the bottom left corner of the component. (a) $a/L = 0.1$ (b) $a/L = 0.25$ (c) $a/L = 0.40$.

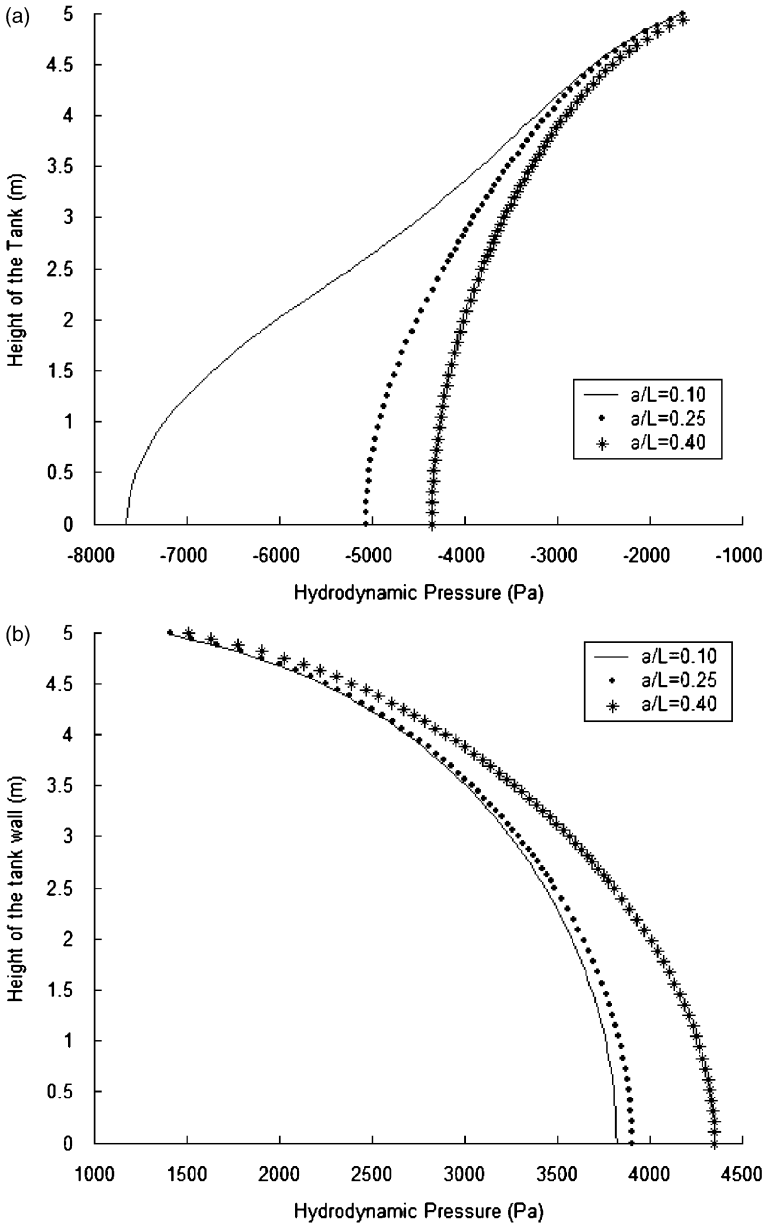

Fig. 17. Hydrodynamic pressure along tank walls: (a) left wall of the tank, (b) right wall of the tank.

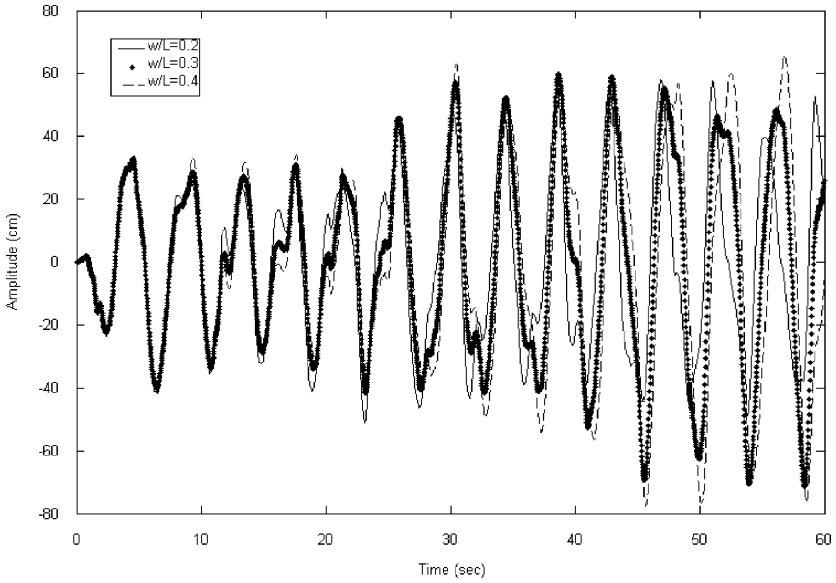

Fig. 18. Free surface wave amplitude variation with time.

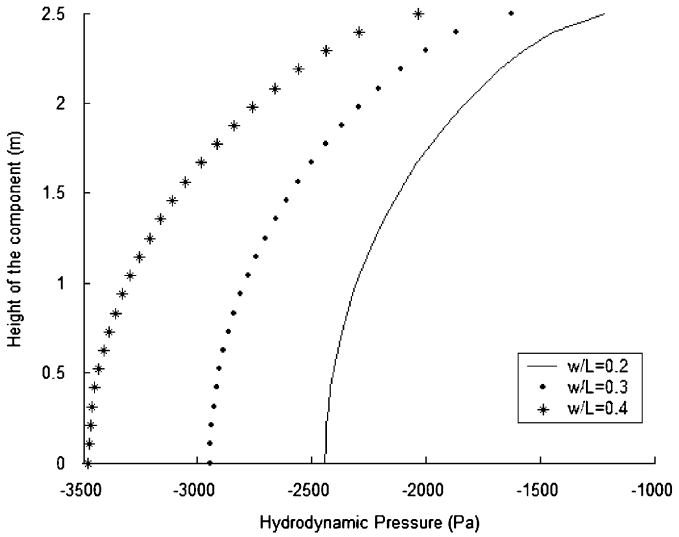

Fig. 19. Hydrodynamic pressure along left wall of the component.

surface wave amplitude increases. The increase is marginal at the initial stage of the response but considerable at a later time. It is also observed from the results that the hydrodynamic pressure on the container and component walls increases with the width of the component. Figs. 19 and 20 show the pressure along the walls of the tank and component due to different width of the component at a particular time instant. The pressure variations at the top and bottom left corner of the component are shown in Figs. 21 and 22. The results show that the pressure increases on both the tank and component walls as the submerged component becomes wider. The temporal variations of the surface wave height at the left and right walls are plotted in Fig. 23 for $w/L = 0.4$ where slosh response is largest. It is found that maximum slosh wave height of about 76 cm occurs at around 46 and 50 s.

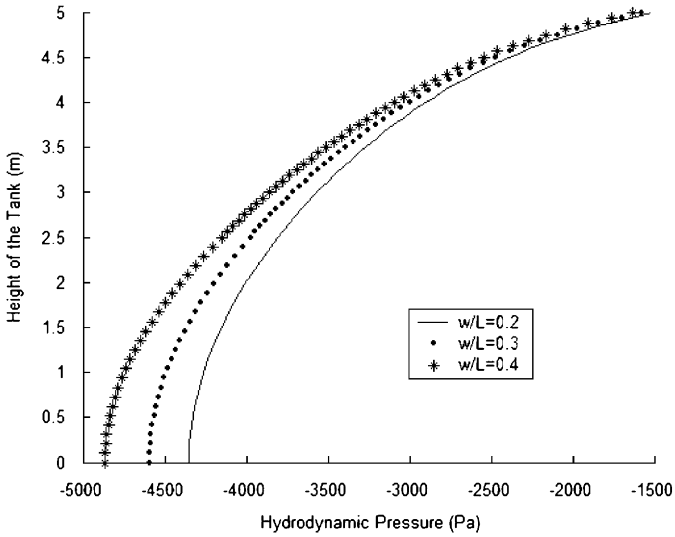

Fig. 20. Hydrodynamic pressure along left wall of the tank.

7. Conclusion

A pressure-based Galerkin's finite element code that can handle liquid sloshing due to free lateral vibration of ground supported rectangular storage tank with submerged internal component has been developed.

The analysis is restricted to linear problems in the sense that only small amplitude waves have been assumed. The method has been applied to a number of problems and some typical results are presented that assess the accuracy and applicability of the method. The pressure formulation has great advantages in the computational aspect compared to the displacement and the velocity potential based formulations. Unlike the displacement formulations, the number of unknown per node in this case is only one. Also, the pressure at the structure-fluid interface is directly obtained which would offer a considerable computational advantage, particularly for a fluid–structure coupled simulation, over those formulations where pressure need to be computed from the solution variables at each time step. Combined effects of these can provide quite considerable savings in memory and cost in a three-dimensional fluid–structure interaction problem. The fluid compressibility comes in a natural way in this formulation and the numerical implementation is quite straightforward and without considerable penalties.

It is found from the study that the height and width of the submerged structure have very strong influence on the slosh dynamics. It is observed that the hydrodynamic pressure on the free surface of the rectangular tank shows considerable variation with time for different width and height of the component. The peak wave amplitude at the wall is found to decrease marginally with the height of the submerged component for the tank system and ground motion considered. It is also observed that with increasing height of the component, the hydrodynamic pressure on the tank wall decreases but increases on the component wall. This implies an increase in the sloshing amplitude near the component structure. When the block becomes broader the peak slosh amplitude is found to increase both at the wall and in the vicinity of the block. Also, with increasing component width, the hydrodynamic pressure increases on both component and container walls. For the rectangular container and external excitation considered in the study the maximum hydrodynamic pressure and the maximum slosh wave height of 76 cm occur at around 45 s from the start of motion for $w/L = 0.4$ and $h/d = 0.5$. The hydrodynamic pressure on the walls also increases as the block becomes broader and taller. For the particular tank system considered here, the

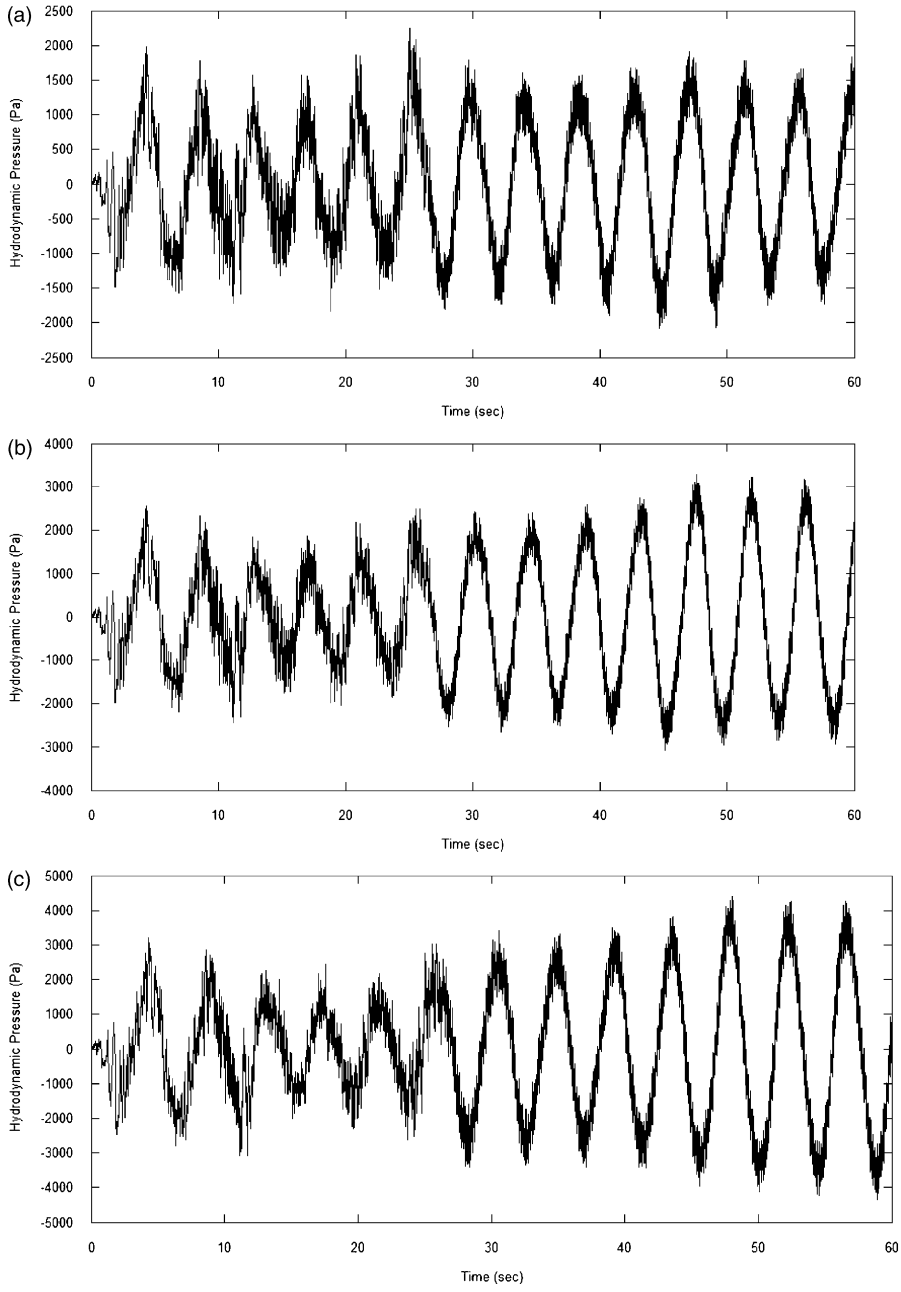

Fig. 21. Hydrodynamic pressure variation at top left corner of the component: (a) $w/L = 0.2$, (b) $w/L = 0.3$, (c) $w/L = 0.4$.

location of the block is found to have much less effect on the sloshing frequencies. However, the dynamic response clearly shows some special features of interests. The peak sloshing amplitude for the off-centered cases does not differ considerably than that of the centered block but the time of occurrence has advanced markedly. The dynamic pressure on one tank wall (the near wall) increases quite considerably as the submerged component moves towards it, while on the other (far) wall the pressure decreases. When the component is quite close to the wall, the pressure on the component walls acts in the same direction for most of the time while it acts in the opposite direction for a component located at the center or very close to the center. The pressure on the near wall of the component, particularly on the lower portion, becomes very large

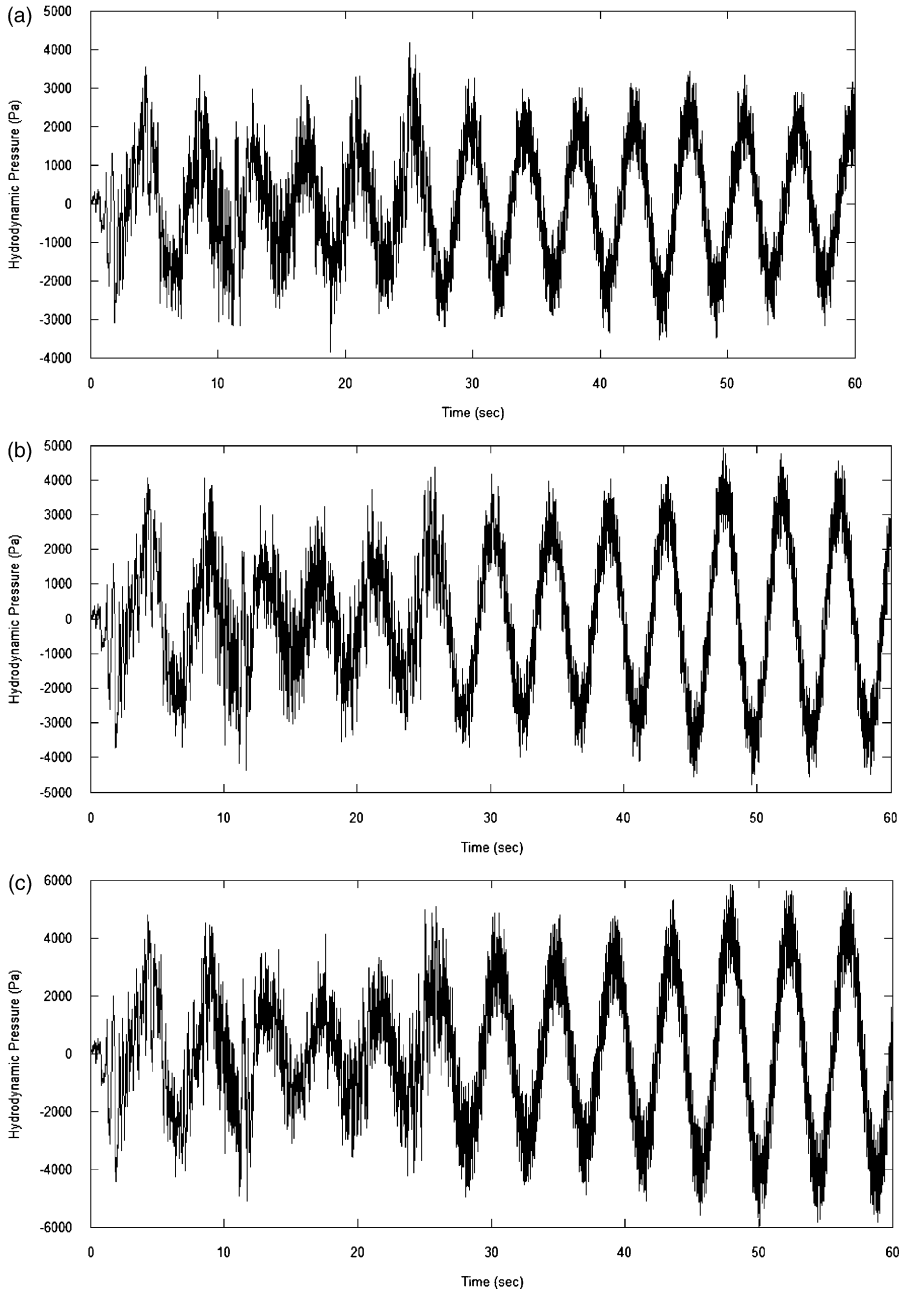

Fig. 22. Hydrodynamic pressure variation at bottom left corner of the component: (a) $w/L = 0.2$, (b) $w/L = 0.3$, (c) $w/L = 0.4$.

during the early stages of the motion when the ground motion also has the largest magnitudes. Subsequently, pressure falls down to more tolerable values albeit considerably higher than that on a central or nearly central block.

The developed computer code is useful in predicting the sloshing displacement, the pressure developed in a liquid-filled container due to sloshing. Information regarding the sloshing displacement is effective in deciding the level of liquid in tanks, fixing the level of an outlet pipe in a boiler suppression pool, etc. The prediction of wall displacement due to sloshing is useful in the design of liquid-filled containers. It is shown that the

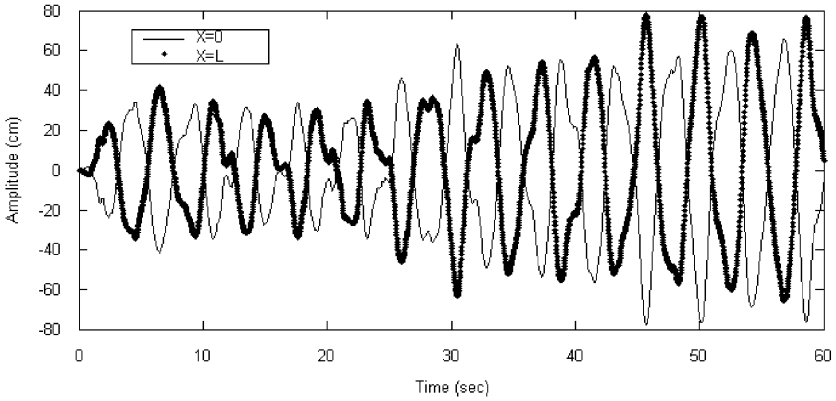

Fig. 23. Time histories of surface wave amplitude at both wall for $w/L = 0.4$.

formulation can be employed with confidence to predict the static and dynamic response of contained fluids with submerged body.

References

[1] Y.S. Choun, C.B. Yun, Sloshing characteristics in rectangular tanks with a submerged block, *Computers and Structures* 61 (3) (1996) 401–413.
[2] Y.S. Choun, C.B. Yun, Sloshing analysis of rectangular tanks with a submerged structure by using small-amplitude water wave theory, *Earthquake Engineering and Structural Dynamics* 28 (1999) 763–783.
[3] O.C. Zienkiewicz, P. Bettes, Fluid–structure dynamic interaction and wave forces—an introduction to numerical treatment, *International Journal for Numerical Methods in Engineering* 13 (1978) 1–16.
[4] K. Washizu, T. Nakayama, M. Ikegewa, Y. Tanaka, T. Adachi, Some finite element techniques for the analysis of nonlinear sloshing problems, in: R.H. Gallaghar (Ed.), *Finite Elements in Fluids*, Vol. 5, Oden, Zenkiewicz, Kawai, Kawahara, 1984, pp. 357–376.
[5] L.G. Olson, K.J. Bathe, A study of displacement-based fluid finite elements for calculating frequencies of fluid and fluid–structure systems, *Nuclear Engineering and Design* 76 (1983) 137–151.
[6] N. C. Pal, Coupled Slosh Dynamics of Liquid Filled Laminated Composite Containers, PhD Thesis, IIT Kharagpur, 1999.
[7] Aslam, Godden, Scalise, Earthquake sloshing in annular and cylindrical tanks, *Journal of Engineering Mechanics ASCE* EM3 (1979) 371–389.
[8] A.S. Veletsos, Seismic response and design of liquid storage tanks, *Guidelines for the Seismic Design of Oil and Gas Pipeline Systems*, Technical Council on Lifeline Earthquake Engineering, ASCE, New York, 1984, pp. 255–364.
[9] E.B.B. Watson, D.V. Evans, Resonant frequencies of a fluid in containers with internal bodies, *Journal of Engineering Mathematics* 25 (1991) 115–135.
[10] W.C. Muller, Simplified analysis of linear fluid–structure interaction, *International Journal for Numerical Methods in Engineering* 17 (1981) 113–121.
[11] S.W. Yuan, *Foundations of Fluid Mechanics*, SI Unit Edition, Prentice-Hall International, Inc., Englewood cliffs, NJ, 1976, pp. 415–416.
[12] J. Lighthill, *Waves in Fluids*, Cambridge University Press, Cambridge, 1978.
[13] MATLAB, The MathWorks, Inc., Natick, MA, July 2002.
[14] K.-J. Bathe, *Finite Element Procedures*, Prentice-Hall of India Private Limited, 1996.
[15] ADINA Users Manual, ADINA Engineering AB, Vasteras, Sweden, 1984.